Int. J. Electrochem. Sci., 16 **(2021)** 150486, doi: 10.20964/2020.10.80

International Journal of
ELECTROCHEMICAL
SCIENCE
www.electrochemsci.org

Cobalt and Nickel Nanoparticles Binary Catalyst Modified Glassy Carbon Electrode for Glucose and Ascorbic Acid Electrooxidation in Alkaline Medium

Mohamed I. Awad[1,2,*], *B. A. Al-Jahdaly*[1], *Omar A. Hazazi*[1] *and Mohammed A. Kassem*[1,3,*]

[1] Chemistry Department, Faculty of Applied Sciences, Umm Al-Qura University, Makkah, Saudi Arabia.
[2] Chemistry Department, Faculty of Science, Cairo University, Cairo, Egypt.
[3] Chemistry Department, Faculty of Science, Benha University, Benha13518, Egypt
[*]E-mail: miawad@uqu.edu.sa and mawad70@yahoo.com (M.I. Awad); makassem@uqu.edu.sa and maa_kassem@hotmail.com (M.A. Kassem)

Received: 6 April 2020 / *Accepted:* 25 May 2020 / *Published:* 30 November 2020

Glucose and ascorbic acid (AA) electrooxidation are examined at a binary catalyst of nickel and cobalt nanoparticles, modified in a certain order onto glassy carbon (GC) electrode. Either nano-Ni was deposited then followed by nano-Co or the reverse. The modified electrodes are characterized morphologically and voltammetrically. The electrochemical response of the nano-Co modified electrodes critically depends on the modification of the underlying substrate. Deposition of nano-Co on a pre-deposited nickel subjected to electrooxidation, designated as nano-Co/NiOx/GC, resulted in a significant catalysis of glucose oxidation. The nano-Co/NiOx/GC electrode is utilized for the simultaneous investigation of glucose and AA using square wave voltammetry (SWV). The linear dynamic ranges for the two species were determined. The LOD and LOQ values were calculated and founded 0.176 and 0.528 μM for AA and 0.066 and 0.199 μM for glucose. Also, the precision of the developed method was evaluated by determining the relative standard deviation (RSD) and found less than 2.3%.

Keywords: Binary electrocatalyst; Cobalt; Nickel; Nanoparticles; Glucose, Ascorbic acid; Voltammetry.

1. INTRODUCTION

Glucose is of pivotal role in physiological processes, and its concentration probing is critically important in many fields [1–3]. It includes, but not limited to, food industry, biomedical and sustainable energy resources. Glucose oxidation has been a basis for the direct and/or indirect way for a glucose probe improvment to monitoring the blood glucose concentration [4–7]. The glucose concentration is

considered as a biomarker for many diseases and disorders. Around 85 % of biosensor research is directed to this area. Therefore, design of a reliable and low-cost glucose sensors to monitor selectively and sensitively glucose levels is of great demand [8]. On the other hand, the coexistence of ascorbic acid (AA), a vital vitamin, with glucose is unavoidable [9,10]. Thus, simultaneous electroanalysis of glucose and AA in biological systems is critically important.

AA coexists with glucose in physiological samples [11], and the determination of both species is interfering as their oxidation peaks cannot be realized at bare electrodes. Modified electrodes can advantageously detect both species selectively via catalyzing any of them and retarding the other. Glucose is usually analyzed based on enzymatic–based or non-enzymatic based electrodes. The enzymatic one passed three generations; the first depends on the presence of glucose-1-oxidase enzyme in addition to oxygen as a co-substrate, the second one is based on using either glucose-1-oxidase (GOx) or glucose dehydrogenase (GDH) in addition to suitable mediator instead of oxygen co-substrate. The electron transfer at the electrode surface was the basis of the third one. Enzymatic analysis for glucose even though it is characterized by high selectivity, but at whole suffers from the bio-compatibility in addition to the difficult immobilization of the enzyme. In addition, every generation suffer from certain drawbacks which were subsequently solved by the next one. The first generation suffer from the possible interfering with coexisting electroactive species and the dependence on oxygen as a co-substrate which might leads to the production of H_2O_2. H_2O_2 able to oxidize at lower potentials and interfere with the analysis [12-15]. The second generation does not solve the problems of the possible interfering of oxygen in addition to the difficult tethering of the mediator and the enzyme at the electrode surface [16-20]. The third one suffers mainly from diffusion process as the active part in the enzyme is covered by a thick protein layer. Recently, using nanostructured modified electrodes are on the way to solve this problem [21,22]. The non-enzymatic methods are advantageous compared with enzymatic methods, as it is characterized by stability. It is considered as the fourth generation for glucose sensors, especially after the spike developing in nanostructured modified electrodes [23]. Those electrodes could offer a selective and sensitive analysis of glucose after solving the problem of fouling of the bare electrodes and enhancing the kinetics of glucose oxidation. Accordingly, the current paper is aimed to the simultaneous fractional electroanalysis of glucose and AA in their coexistence via tailoring suitable nanoparticles on carbon electrodes or suitable underlying substrate. The nanoparticle integration of cobalt and nickel is of major importance because of their peculiar catalytic activity compared with their bulk electrodes' counterparts. Tailored fabrication of nanostructured modified electrodes could introduce the plethora of sensitive and selective response of a sensor. Thus, the present work aims at the fabrication of a cost-effective sensor for the simultaneous analysis of glucose and ascorbic acid, i.e., non-enzymatic sensor to avoid the disadvantage of biocompatibility and difficult setting.

2. EXPERIMENTAL

2.1. Reagents and chemicals

Sulphuric acid (H_2SO_4), ascorbic acid, glucose, cobalt chloride hexahydrate ($CoCl_2.6H_2O$), nickel chloride hexahydrate ($NiCl_2.6H_2O$), nickel sulphate heptahydrate ($NiSO_4.\ 7H_2O$) and other analytical grade chemicals were purchased from Sigma-Aldrich and used without further purification.

Bidistilled water was used thorough the experiments. Ascorbic acid solutions were freshly prepared as daily required. Boric acid was obtained from BDH Chemicals Ltd Poole England. Phosphate buffers were prepared using NaH_2PO_4 and Na_2HPO_4 salts, obtained from BDH [24].

2.2. Pretreatment of working electrodes

The glassy carbon electrode of 3 mm diameter (GC) was polished with fine alumina powder, rinsed with water and then was subjected to sonication for removal of alumina. Then, GC was either used directly or after electroactivation by cycling the potential of the electrode in the potential range -0.2 to 2 V for 5 potential cycles. The anodic oxidation of GC in H_2SO_4 results in an increase of the percentage surface composition of functional groups bearing –OH group. The presence of –OH group adsorbed on the GC surface (i.e., OH_{ads}) promotes the electrocatalytic oxidation of glucose and other small organic molecules such as methanol [25-27].

2.3. Preparation of modified electrodes

Cobalt nanoparticles (Nano-Co) were electrodeposited from 5 mM $CoCl_2$ in 0.1 M boric acid solution, onto glassy carbon (GC) electrodes by scanning potential from 0.5 to -1.0 V. Nano-Co either deposited on GC or on pre-electrodeposited nickel nanoparticles which were deposited from 0.02 M $NiSO_4$/ 0.02 M $NiCl_2$ in 0.1 M boric acid applying a potential scan in the range from 0.5 to -1.0 V. This obtained modified electrode will be designated as nano-Co/NiOx/GC. For electrodeposition of both cobalt and/or nickel, different loading cycles were performed to deduce the optimum one.

2.4. Measurements

Electrochemical measurements were conducted using Autolab PGSTAT30 potentiostat/galvanostat with a compliance voltage of 30 V and a bandwidth of 1 MHz from Metrohm. An Ag/AgCl (KCl sat.) electrode, from Sigma-Aldrich, was used as the reference electrode. A conventional three-electrode cell was used for all measurements. Jeol JSM 6400 system were used for scanning electron microscope (SEM) micrographs and energy-dispersive X-ray spectroscopy (EDX) spectra. The electron energy used was 20 keV. X-ray diffraction (XRD) measurements were performed using Philips PW 1700 powder X-ray diffractometer using Cu Ka1 radiation with a Ni filter working at 40 kV and 30 mA.

3. RESULTS AND DISCUSSION

3.1. Electrode modification:

Fig. 1. displays CV obtained at (a) GC in 0.1 M boric acid containing 5 mM Co^{2+}, (b) GC in 0.1 M boric acid containing 5 mM Co^{2+} + 20 mM Ni^{2+} and (c) nano-Ni/GC in 0.1 M boric acid containing 20 mM Ni^{2+}. Nano-Ni/GC was fabricated by applying a potential scan in the range from 0.5 to -1.0 V. Curve b represents the simultaneous deposition of cobalt and nickel and curve c represents the deposition

of cobalt on previously deposited nickel. The behavior is different denoting that the amount of deposition as well as the morphology are different, and this should be reflected on the morphology as shown in Fig. 2 shown hereafter. In the case of the simultaneous deposition (curve b), no peak for the reduction is revealed, similar to the direct deposition of Co on GC (curve a). In the deposition of cobalt on GC (curve a) or on Ni/GC (curve c) the nucleation loop shows a peak at around -0.78 V, pointing to different mode of deposition in this case.

In the cathodic sweeping of potential towards the negative direction, the cathodic current rise around - 0.78V (curves b and c), and little bit delayed in the case of the direct deposition on GC substrate (curve a). Then it keeps going to raise because of the accumulation of deposited Co [28]. The vertex potential is limited to -1.0 V as the hydrogen evolution interfere with cobalt deposition. In the anodic scanning, a crossover potential, occurs between the cathodic and anodic current traces, resulting in a nucleation loop which is observed at around - 0.8 V. This crossover of potential is attributed to the extensive change in the surface of the underlying substrate due to the deposition of cobalt [29,30]. It can be attributed also to the difference in deposition and dissolution potentials [31]. The presence of the crossover is diagnostic for the nuclei formation on the electrode. It occurs at a current around zero current, i.e., at a nucleation rate of almost zero consistent with literature [32]. The cathodic current is coupled with two anodic peaks (at around - 0.1 and 0.04 V) in the cases of direct deposition of Co onto GC (curve a) and of deposition on pre-deposited nickel (curve b). This probably correspond to the dissolution of the different cobalt phases [33-36]. In the case of the simultaneous deposition of both species, anodic peaks appeared at relatively large anodic potentials. This points to a different extent of deposition in this case compared with the other two cases. Thermodynamically, it is expected that Ni deposition (E^o = -0.25 V) starts at more noble potentials than cobalt (E^o = -0.28 V). However, in the present case depositing both species individually shows preferential deposition of cobalt. This attitude might be referred to kinetical restriction [37].

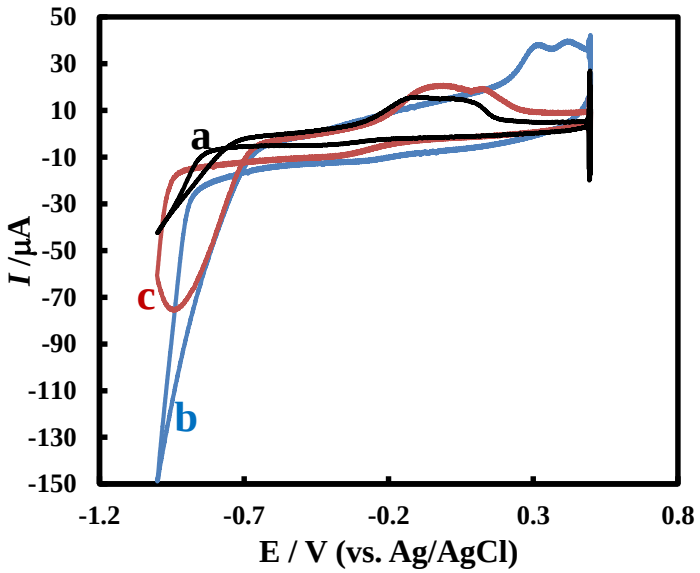

Figure 1. CV obtained at (a) GC in 0.1 M boric acid containing 5 mM Co^{2+}, (b) GC in 0.1 M boric acid containing 5 mM Co^{2+} + 20 mM Ni^{2+} and (c) nano-Ni/GC in 0.1 M boric acid containing 5 mM Co^{2+} (scan rate of 100 mV/s).

3.2. Morphological investigation:

Fig. 2 demonstrates the SEM images for the electrodes prepared as represented in Fig. 1 shown above; i.e., (A) nano-Ni/GC, (B) nano-Co-Ni/GC and (C) nano-Co/NiO_x/GC electrodes. In image A, a deposition of particles of around 20 nm of nickel are shown. In image B (for nano-Co-Ni/GC), a uniform deposition of particles of size around 18 nm are obtained. In image C (obtained for nano-Co/NiO_x/GC) in which nano-Ni after being deposited onto GC is subjected to electrooxidation and subsequently cobalt is deposited a relatively smaller particles of ca. 11 nm are obtained.

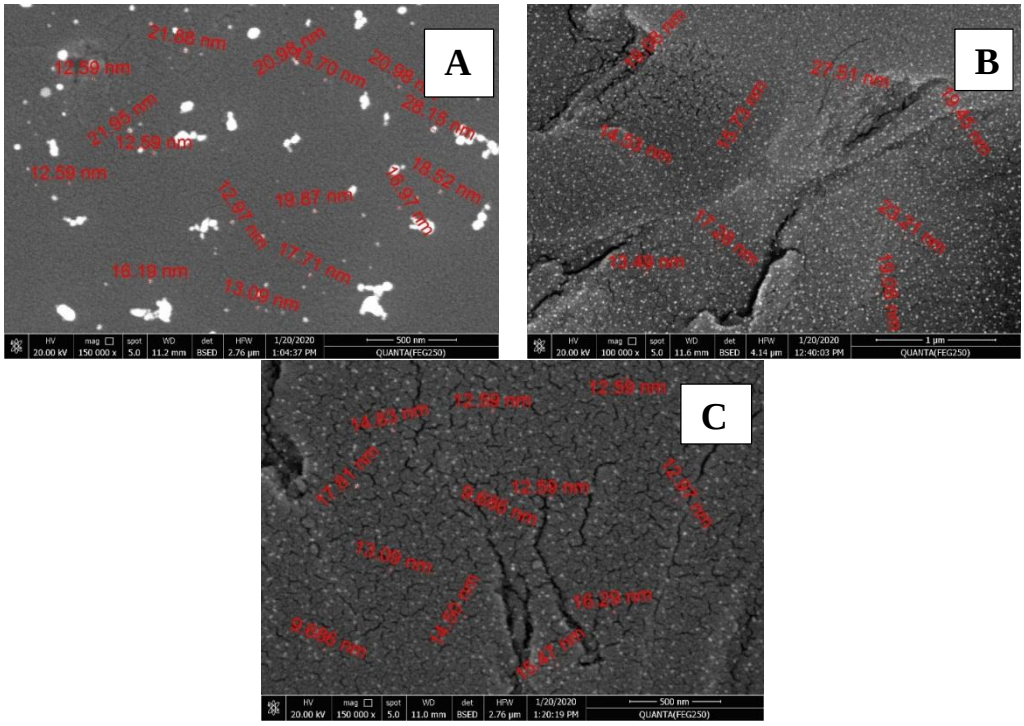

Figure 2. SEM images for the prepared electrodes where (A) nano-Ni/GC, (B) nano-Co-Ni/GC and (C) nano-Co/NiOx/GC electrodes.

The elemental analysis of the modified electrodes is probed by EDX as shown in Fig. 3 in which EDX analysis for (A) nano-Ni/GC, (B) nano-Co-Ni/GC and (C) nano-Co/NiOx/GC electrodes are given. The nickel signal appeared clearly in Figure A at 8.2, 7.7, and 0.9 KeV. In panels B (nano-Co-Ni/GC) and C (Co/NiOx/GC) the signals of nickel is largely suppressed. This might be due to the deposition of cobalt atop the pre-deposited nickel.

The crystallinity of the deposited nanoparticles was assessed using X-ray diffraction (XRD) shapes. Fig. 4 displays XRD analysis for the prepared electrodes where (A) nano-Ni/GC, (B) nano-Co-Ni/GC and (C) nano-Co/NiOx/GC electrodes. In spectrum (A), distinctive peaks of NiOx found at $2\theta = 37°$, 43°, 44°, 74° and 76° may be clearly referred to (101), (012), (111), (220) and (202) crystal faces of the NiO_x, respectively. Those peaks are indexed to the face-centered cubic (FCC) crystalline structure of NiOx in accordance with that of the standard spectrum (JCPDS, No. 04-0835) [38]. The hydroxides

of Ni and Co possessing two α and β phases of hexagonal-layered structure, respectively. The peaks at about 19°, 33° and 38° are attributed to the (001), (100), (002), respectively, of β phase.

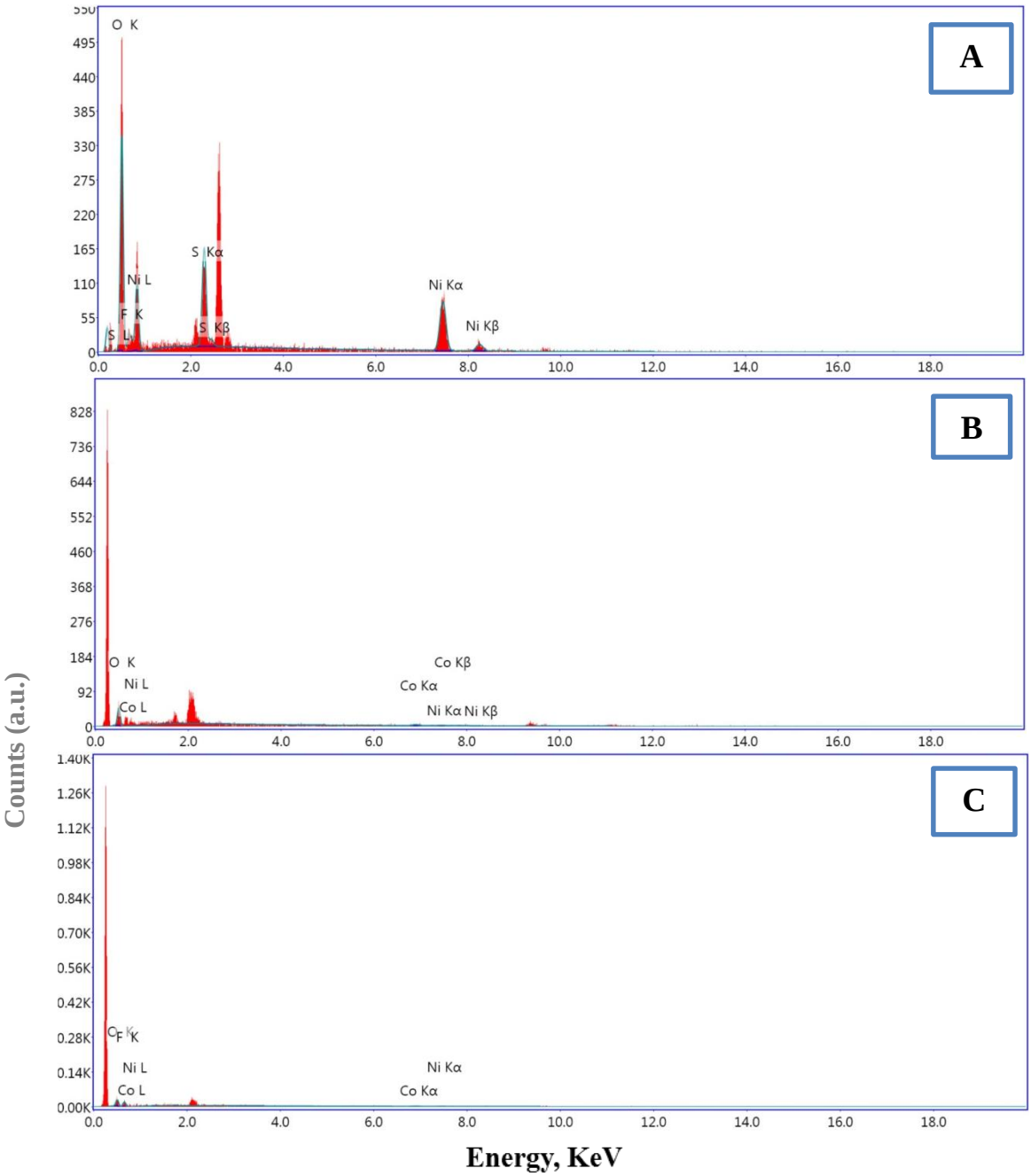

Figure 3. EDX analysis for the prepared electrodes where (A) nano-Ni/GC, (B) nano-Co-Ni/GC and (C) nano-Co/NiOx/GC electrodes.

The peaks for alpha phase are not revealed. The two peaks at angles larger than 70 corresponds to the oxide formed upon oxidation of electrode [39] The characteristic peaks at $2\theta = 21°$, 37°, 42°, 53°, 70° and 77 for cobalt oxide nanoparticles, which are marked respectively by their indices (111), (220), (311), (400), (511) and (440) in agreement with JCPDS card no 73-1701. These XRD data give an evidence for the formation of nano-Co [40,41].

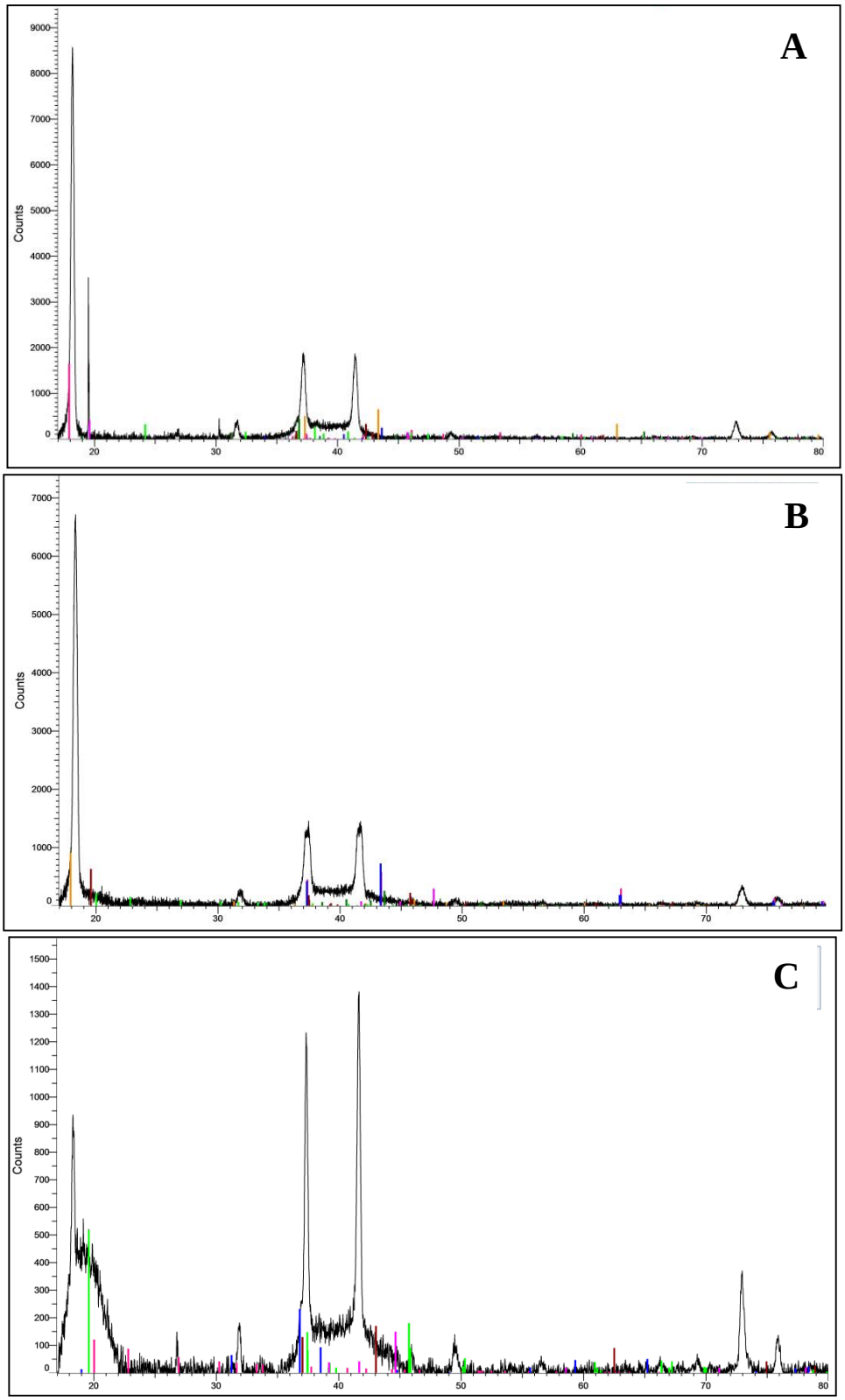

Figure 4. XRD analysis for the prepared electrodes where (A) nano-Ni/GC, (B) nano-Co-Ni/GC and (C) nano-Co/NiOx/GC electrodes.

3.3. Electrocatalysis and Electroanalysis:

Fig. 5. Shows CVs obtained at (a) nano-Ni/GC, (b) nano-Co-Ni/GC and (c) nano-Co/NiOx/GC electrodes in 0.1 M NaOH, at a scan rate of 100 mV/s. Ni was deposited on GC (curve a) and subsequently either Co was deposited on the thus deposited nickel (b) directly or after (c) oxidation of nickel. As clearly shown;

- The nickel couple is clearly shown at nano-Co/NiOx/GC compared with that at nano-Ni/GC. In addition, the anodic peak is very sharp pointing to the enhancing kinetics in this case. As shown in Fig. 5, the Co/GC shows several couples. Probably, the intense peak is a combination of that of Co and Ni.
- The couple of the nickel is preceded by a tenuous increase in the current, likely this corresponds to the deposited cobalt.
- The couple is obtained at lower potential compared with those obtained at nano-Ni/GC and nano-Co-Ni/GC.

while the deposition of Ni onto Co/GC results in a voltammetric behavior combine both couples of cobalt and nickel with comparable intensities, when the order is reversed, i.e., Ni is deposited first followed by cobalt, the response for nickel is extensively larger than that of cobalt. This is an interesting behavior which needs further investigation, and it is underway.

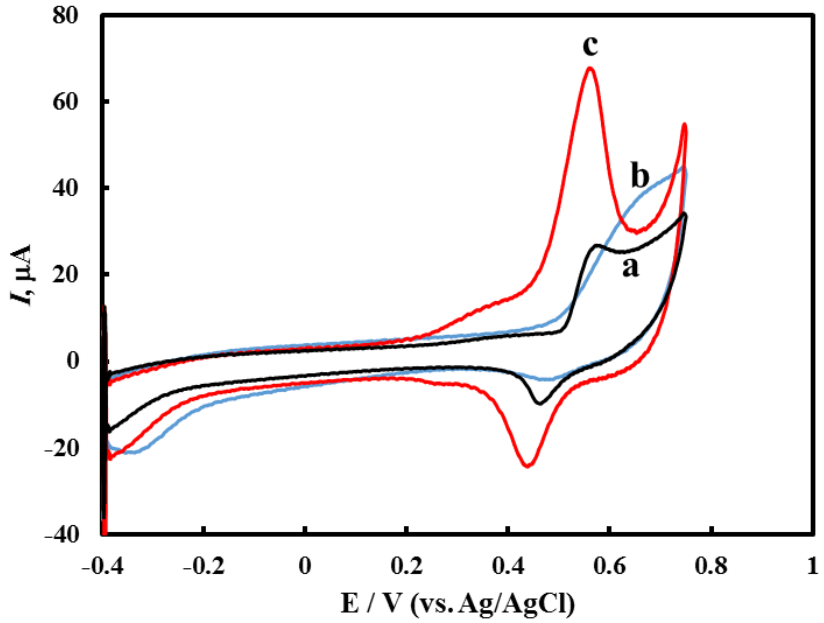

Figure 5. XRD analysis for the prepared electrodes where (A) nano-Ni/GC, (B) nano-Co-Ni/GC and (C) nano-Co/NiOx/GC electrodes.

Fig. 6 shows CVs for 2 mM Ascorbic acid and 2.5 mM Glucose at the modified electrodes, i.e., at (a) nano-Ni/GC, (b) nano-Co-Ni/GC and (c) nano-Co/NiOx/GC (scan rate of 100 mV/s). In curve (a) obtained at nano-Ni/GC, the oxidation peaks for glucose and AA are shown at 0.6 and - 0.1 V,

respectively. The one for AA is not well defined and the one for glucose shown the crossing in the CV. The mediation of glucose oxidation is clearly revealed as the cathodic peak of the nickel couple (shown in Fig. 4) almost vanished while the anodic one significantly increased. At nano-Co-Ni/GC (curve b), the response for the two species become less defined and retarded. At nano-Co/NiOx/GC (curve c), interestingly, the anodic peak of glucose appeared clearly at 0.54 V. In addition, the anodic peak of AA is obviously shown at -0.1 V. Both peaks are revealed with a very large separation of their peak potential which could enable in the simultaneous analysis of both species in their coexistence.

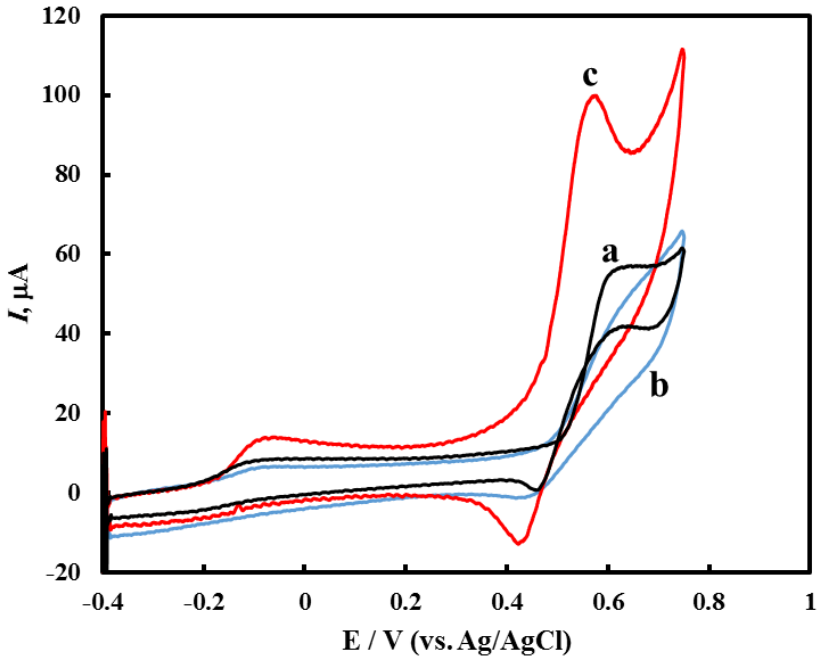

Figure 6. CV for 2 mM Ascorbic acid and 2.5 mM Glucose on the modified electrodes in 0.1 M NaOH where (a) nano-Ni/GC, (b) nano-Co-Ni/GC and (c) nano-Co/NiOx/GC (scan rate of 100 mV/s).

Fig. 7. Shows CV obtained at nano-Co/NiOx/GC electrode in (a) 0.1 M NaOH containing constant concentration of AA and different concentration of glucose. Comparing curves, a and b, the two peaks of AA and glucose are clearly revealed at - 0.1 and 0.51 V, respectively. Comparing curves b, c and d confirms the correspondence of these two peaks; the peak at – 0.1 V correspond to AA oxidation remains constant, while that at around 0.51 V (corresponds to glucose oxidation) increases regularly (compare curves c and d). It reveals clearly the selectivity of the present electrode for the simultaneous determination of glucose and AA accurately and precisely.

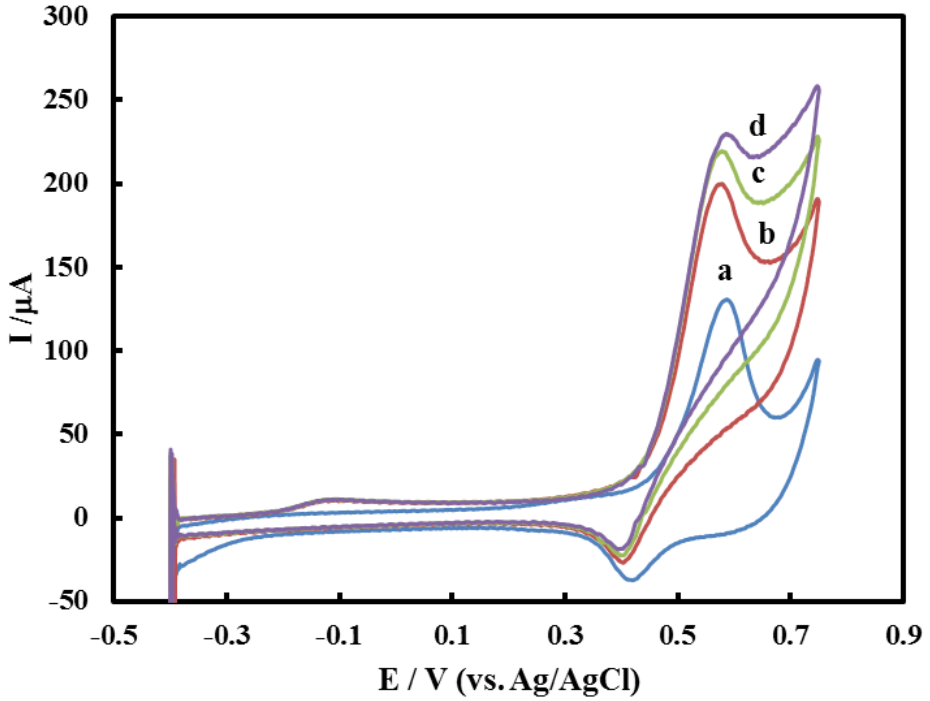

Figure 7. CV obtained at nano-Co/NiOx/GC electrode in (a) 0.1 M NaOH containing (b) 1 mM Ascorbic acid + 2.5 mM Glucose, (c) 1 mM Ascorbic acid + 5 mM Glucose and (d) 1 mM Ascorbic acid + 7.5 mM Glucose. Scan rate of 100 mV/s.

3.4. Electroanalysis of AA and glucose using nano-Co/NiOx/GC electrode

Figure 8 shows the square wave voltammetry (SWV) acquired at nano-Co/NiOx/GC for AA and glucose. The calibration graph extracted from these square wave voltammograms were presented in Fig. 9. The calibration curves for AA and glucose were in a linearity in ranges of 0.65-6.5 and 0.84-8.4 mM for AA and glucose, respectively. These calibration curves were in a good correlation coeffiecents (R^2) of 0.9936 and 0.9996. The regration relation for these lines were:

I(µA) =8.6499 [AA](mM) + 1.7467 ……(1)

I(µA) =s15.517 [glucose](mM) – 1.1733……(2)

The limits of detection (LOD) and limit of quantitation (LOQ) were calculated utalizing the formula kS_b/m [42], where, S_b is the standard deviation of the blank response (n = 6), m is the slope of the calibration curve and k = 3.3 for LOD and 10 for LOQ. The LOD and LOQ values were calculated and founded 0.176 and 0.528 µM for AA and 0.066 and 0.199 µM for glucose. These values indicated the sensitivity of the modified method for accurate determination of both analytes. The standard deviation and the relative standard deviation for six replicate measurements for 5.0 mM concentration for both AA and glucose were calculated, and the results were summarized in Table 1. As it can be seen, the proposed method has a wider linear range than those reported for AA and glucose determination. Table 2 represented a comparison of the voltammetric determination for AA and glucose in the present work and some recent reported methods. The obtained dynamic linear ranges and the detection limits are in reasonable values with most compared ones.

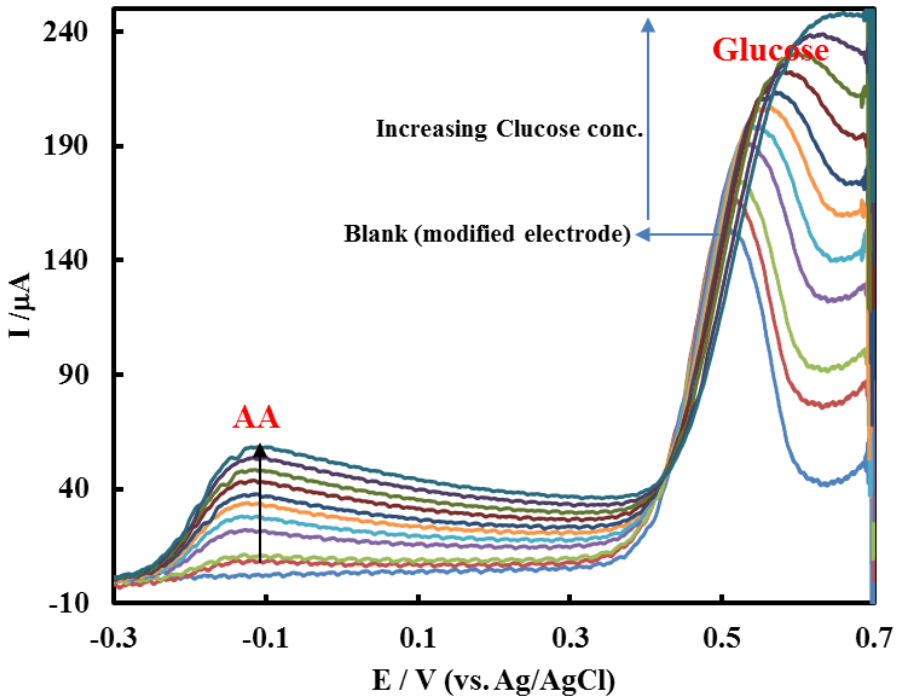

Figure 8. SWV obtained at nano-Co/NiOx/GC in 0.1 M NaOH containing different concentrations of AA (0.65-6.5 mM) and glucose (0.84-8.4 mM), Scan rate: 100 mV/s.

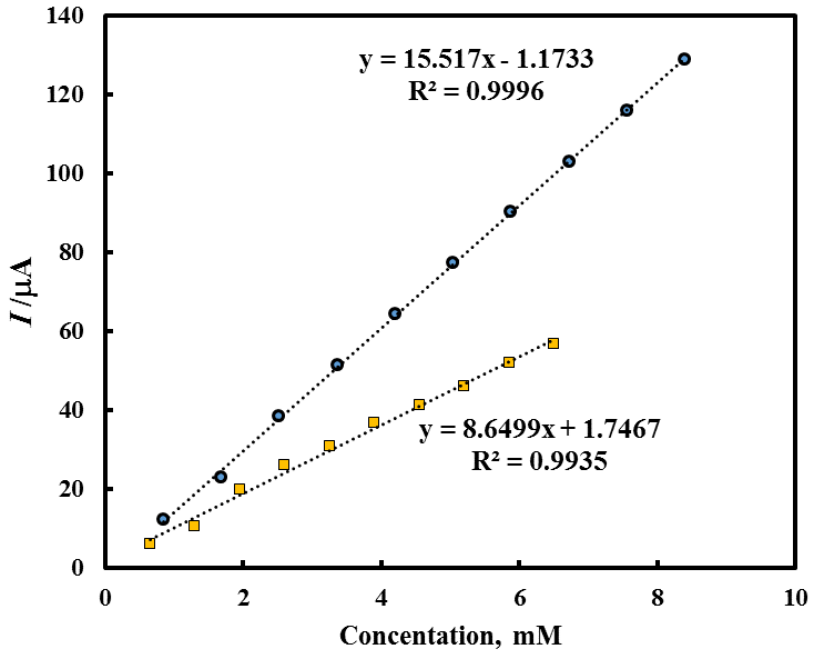

Figure 9. Calibration curves for electroanalytical determination of AA and glucose using the data obtained from Fig. 8.

Table 1. The optimum conditions and the analytical parameters for the simultaneous determination of AA and glucose using the electrode under study.

Parameters	AA	Glucose
Media for measurment	0.1 M NaOH	0.1 M NaOH
Potential of measurment, V	-0.1	0.5
Scan rate, mV sec^{-1}	100	100
Linear concentration range, mM	0.65-6.5	0.84-8.4
Regression equation[a]		
Slope, µA/mM	8.6499	15.517
Intercept, µA	1.7467	-1.1733
Correlation coefficient, R^2	0.9936	0.9996
Standard deviation, SD (n=6), mM	0.11	0.09
Relative standard deviation, RSD[b], %	2.2	1.8
LOD, µM	0.176	0.066
LOQ, µM	0.528	0.199
SD of slope	0.108	0.049
SD of intercept	0.462	0.313

[a] I(µA) =slope [Analyte](mM) ± Intercept

[b]Average of six consecutive measurements.

Table 2. Comparison for voltammetric determination for glucose and AA with the proposed method.

The technique used	The electrode used	Linear range, mM		Detection limit, µM		Ref.
		Glucose	AA	Glucose	AA	
DPV	NiO/GO/GCE.	--	40-700	--	5.50	[43]
DPV	The gold nanotube arrays/GCE	--	0.01-5.23	--	1.12	[44]
SWV	Imprinted copolymer of o-phenylenediamine and pyrrole on pencil graphite electrode	--	0.01-1.0	--	0.263	[45]
DPV	Cu-based NPs@3DG	0.8-10	--	16	--	[46]
AMP	Ni/Cu/CNTs	0.02-4.5	--	2.0	--	[47]
CHOR	Chitosan/glucose oxidase/Prussian blue-graphite modified GCE	0.015-1.5	--	5.7	--	[48]
SWV	Nano-Co/NiOx/GCE	0.84-8.4	0.65-6.5	0.066	0.176	PM

DPV: Differential pulse voltammetry, AMP: Amperometry, PM: Present method
SWV: Squre wave voltammetry, CHOR: Chronoamperometry, GCE: Glassy carbon electrode

4. CONCLUSIONS

Glucose and AA are simultaneously analyzed at nano-Co/NiOx/GC, in which nickel deposited onto GC (nano-Ni) is subjected to electrochemical oxidation in alkaline medium and subsequently cobalt is deposited on nano-Ni. The modified electrode is characterized morphologically and electrochemically. Under the optimum conditions and using a well modified nano-Co/NiOx/GC electrode, the SWV technique was successfully performed for electroanalysis of AA and glucose. The two tested species were determined within a dynamic ranges 0.65-6.5 mM and 0.84-8.4 mM for AA and glucose, respectively. The developed method had a high

sensitivity with low limit of detections. A low RSD of 2.2 and 1.8% for the two species, respectively, indicated the high precise of our method.

ACKNOWLEDGEMENTS
The Authors would like to thank the Deanship of Scientific Research at Umm Al-Qura University for supporting this work by Grant Code: 17-SCI-1-01-0016.

References

1. A.L. Galant and R.C. Kaufman, *Food Chem*., 188 (2015) 149.
2. F. Ricci, A. Amine, G. Palleschi and D. Moscone, *Biosens. Bioelectron*., 18 (2003) 165.
3. S. Wang, Y. Tan, D. Zhao and G. Liu, *Biosens. Bioelectron*., 23 (2008) 1781.
4. J. Qian, Y. Wang, J. Pan, Z. Chen, C. Wang, J. Chen and Z. Wu, *Mater. Chem. Phys.*, Volume 239, 1 January 2020, 122051.
5. M.C. Tsai. and Y.C Tsai, *Sens. Actuators B Chem*., 141 (2009) 592.
6. D. Feng, F. Wang and Z. Chen, *Sens. Actuators B Chem*., 138 (2009) 539.
7. P. Balasubramanian, M. Velmurugan, S.M. Chen and K.Y. Hwa, *J. Electroanal. Chem.*, 80715 (2017) 128.
8. C.G. Caridade, R. Pauliukaite and C.M.A. Brett, *Electrochim. Acta*, 53 (2008) 6732.
9. M. Shamsipur, M. Najafi and M.R. Hosseini, *Bioelectrochem*., 77 (2010) 120.
10. C. Wang, R. Yuan, Y. Chai, S. Chen, F. Hu and M. Zhang, *Anal. Chim. Acta*, 741 (2012) 15.
11. R. Ojani, J.B. Raoof and S.R.H. Zavvarmahalleh, *Electrochim. Acta*, 53 (2008) 2402.
12. A.A. Ensafi, M. Taei and T. Khayamian *Colloids Surf*., B, 79 (2010) 480.
13. I. Jeerapan, J.R. Sempionatto, J.M. You and J. Wang, *Biosens. Bioelectron.*, 12230 (2018) 284.
14. J.C. Armour, J.Y. Lucisano, B.D. McKean, and D.A. Gough, *Diabetes*, 39 (1990) 1519.
15. J. Wang and F. Lu, *J. Am. Chem. Soc*., 120 (1998) 1048.
16. J. Wang, J.W. Mo, S. Li, and J. Porter, *Anal. Chim. Acta*, 441 (2001) 183.
17. S. Tsujimura, S. Kojima, K. Kano, T. Ikeda, M. Sato, H. Sanada and H. Omura, *Biosci., Biotechnol., Biochem.*, 70 (2006) 654.
18. A. Suzuki, N. Mano and S. Tsujimura, *Electrochim. Acta*, 2321 (2017) 581.
19. K. Lau, S.A.L. de Fortescu, L.J. Murphy, and J.M. Slater, *Electroanalysis.*, 15 (2003) 975.
20. Z. Liang, J. Zhang, C. Wu, X. Hu, Y. Lu, G. Wang, F. Yu, X. Zhang and Y. Wang, *Biosens. Bioelectron.*, 1551 (2020) 112105.
21. A. Heller and B. Feldman, *Acc. Chem. Res*., ACS. (2010) ASAP
22. S. Wu, H. Ju, and Y. Liu, *Adv. Funct. Mater*., 17 (2007) 585.
23. S. Chen, R. Devasenathipathy, S. Wang and K. Kohilarani, *Int. J. Electrochem. Sci*., 11 (2016) 5416.
24. D.D. Perrin and Boyd Dempsey, Buffers for pH and Metal Ion Control, (1974) Chapman and Hall Ltd. P. 138.
25. S. Stevanovic, V. Panic, D. Tripkovic and V.M. Jovanovic, *Electrochem. Commun*., 11 (2009) 18.
26. T.S. Sunil Kumar Naik, S. Saravanan, K.N. Sri Saravana, U. Pratiush, P.C. Ramamurthy, *Mater. Chem. Phys.*, 24515 (2020) 122798.
27. M.W. Hsiao, R.R. Adzic and E.B. Yeager, *Electrochim. Acta*. 37 (1992) 357.
28. L. H. Mendoza-Huizar, J. Robles and M. Palomar-Pardave, *J. Electroanal. Chem*., 2002, 521, 95.
29. S. Fletcher and T. Lwin, *Electrochim. Acta.*, 28 (1983) 227.
30. A.C. Frank and P.T.A. Sumodjo, *Electrochimica Acta*., 132 (2014) 75.
31. Southampton Electrochemistry Group, in T.J. Kemp (Ed.), Instrumental Methods in Electrochemistry, Ellis Horwood Ltd, Chichester, UK, 1985.

32. S. Fletcher, C.S. Halliday, D. Gates, M. Westcott and T.L.G. Nelson, *J. Electroanal. Chem*., 159 (1983) 267.
33. R. Bertazzoli and D. Pletcher, *Electrochim. Acta.*, 38 (1993) 671.
34. N.V. Myung, D.Y. Park, B.Y. Yoo and P.T.A. Sumodjo, *J. Magn. Magn. Mater*., 265 (2003) 189.
35. A.B. Soto, E.M. Arce, M. Palomar-Pardavé and I. González, *Electrochim. Acta*, 41 (1996) 2647.
36. S.S. Abd El Rehim, S.M. Abd El Wahaab, M.A.M. Ibrahim and M.M. Dankeria, J. *Chem. Technol. Biotechnol.*, 73 (1998) 369.
37. A. Dolati, M. Sababi, E. Nouri and M. Ghorbani, *Mater. Chem. Phys*., 102 (2007) 118.
38. Y. Ren and L. Gao, *J. Am. Ceram. Soc.*, 93 (2010) 3560.
39. J.S. Hong, J. Pyun, Y.W. Park, C.S. Kim and I.B. Sh, *IEEE Trans. Magn.*, 45 (2009) 2464.
40. JCPDS international center for diffraction data (1991)
41. S. Chattopadhyay, S.P. Chakraborty, D. Laha, R. Baral, P. Pramanik and S. Roy, *Cancer Nanotechnol.*, 3 (2012) 13.
42. F.H. Chen, Q. Gao and J.Z. Ni, *Nanotechnology*, 19 (2008) 165103.
43. J. Gao, P. He, T. Yang, L. Zhou, X. Wang, S. Chen, H. Lei, H. Zhang, B. Jia and J. Liu, *J. Electroanal. Chem.*, 852 (2019) 113516.
44. G. Yang, L. Li, J. Jiang and Y. Yang, *Mater. Sci. Eng., C*, 32 (2012) 1323.
45. C. Yan, X. Liu, R. Zhang, Y. Chen and G. Wang, *J. Electroanal. Chem.*, 780 (2016) 276.
46. Z. Khosroshahi, F. Karimzadeh, M. Kharaziha and A. Allafchian, *Mater. Sci. Eng., C*, 108 (2020) 110216.
47. S.A. Shabbir, S. Shamaila, N. zafar, A. Bokhari and A. Sabah, *J. Phys. Chem. Solids*, 120 (2018) 12.
48. A. Soleh, P. Kanatharana, P. Thavarungkul and W. Limbut, *Microchem. J.*, 153 (2020) 104379.